

OPTIMAL BEAMFORMING AND DEPLOYMENT OF MILLIMETER-WAVE DRONE BASE STATIONS

Tolga Girici¹ and Fatih Yürekli¹

¹Dept.of Electrical and Electronics Eng., TOBB University of Economics and Technology, Ankara, Turkey

NOTE: Corresponding author: Tolga Girici, tgirici@etu.edu.tr

Abstract – Due to their flexible deployment and line-of-sight channel conditions, using drones as base stations is a promising technology. Recent developments in Massive MIMO transmission with millimeter-wave beamforming also enables high data rates and enables simultaneous transmission to multiple ground users. In this work we consider the problem of deployment (i.e. positioning) of drone base stations for maximizing proportional fairness, along with analog MIMO beamforming that maximizes the Signal to Interference plus Noise Ratio (SINR). Simulation results reveal that careful K-means clustering of ground users and altitude adjustment performs close to a Particle Swarm Optimization (PSO)-based solution. Discrete Fourier Transform (DFT) codebook-based low-complexity beamforming also provides a promising performance, when compared to the Semi-Definite Programming (SDP)-based solution, as the number of antennas is increased.

Keywords – Beamforming, deployment, drone base station, mmWave, UAV

1. INTRODUCTION

1.1 Motivation

Unmanned Aerial Vehicles (UAVs), also generally known as drones, have great potential to be used in numerous applications such as surveillance, shipping/delivery and search/rescue operations [1]. What makes it appealing is that besides its small size, it is easily affordable and quickly deployable anywhere. Because of these features, UAVs gain great interest from the wireless communication community [2].

UAVs also have changed the way we think about cellular communications by assisting communication infrastructure and disseminating and collecting data as in the Internet of Things (IoT). Also, using UAV as a base station is standardized by third Generation Partnership Project (3GPP) and Google Loon-enabled emergency LTE services. This usage shows good coverage but limited bandwidth [3]. With 5G and mmWave communications UAVs will gain great importance as Mobile Base Stations (MBSs) especially when terrestrial base stations become out of service or for places that become temporarily crowded such as stadiums or concert halls. They can also be often used by search and rescue units, police and gendarmerie, which may need temporary coverage.

Drone Base Stations (DBSs) have been a very popular research topic in recent years. Deployment and optimal 3-dimensional positioning of the DBSs is one of the most popular problems for research studies [4]. However most of these previous works usually assume a single directional antenna at the DBS and a conventional (e.g. < 6GHz) transmission frequency. For conventional cellular systems the channel model is well-established but these models are often not applicable for UAV mmWave channels [5]. Due to high frequency, Line-of Sight (LoS)

is needed for reliable transmission with a high data rate. Thanks to the height of the DBS, a strong Line-of-Sight is possible. Besides, due to the small wavelength at the mmWave, a large number of antennas can be fit into a small area which makes massive Multiple Input-Multiple Output (MIMO) feasible. However, a large number of antennas brings a challenge in training and channel estimation. In [6], authors describe that the mmWave channel has spatial sparsity in the angle domain and a limited number of multipath components. Under this condition several beamforming techniques are developed. Using mmWave bands provides a large bandwidth and a very high data rate. However, due to mobility of the DBS there is a fast variation of path gain and beam Angle of Arrival (AoA) and Angle of Departure (AoD). In addition to this, in [3] authors state an additional challenge. The selected optimal beam can turn out to be suboptimal due to displacement of a UAV when it is in hover position. Another challenge for the DBSs is the size, weight and power. Due to its lower number of RF-chain requirements and less power consumption, analog beamforming is preferred in UAV-based communications [7], [8]. Due to the mobility, flexible beamforming techniques are required [9]. To fill this gap in the literature, we consider the problem of joint DBS deployment and analog beamforming in millimeter-wave MIMO drone base stations.

1.2 Related works

In the literature there are several pieces of work that address the problem of DBS deployment. In [6] the authors consider a system with single DBS and they utilize approximate beam patterns to simplify the beamforming problem. They use meta-heuristic methods and exhaustive searches to solve the joint problem of deployment and beamforming. The work in [10] considers a single DBS system with Uniform Linear Array (ULA) antennas

and utilized learning methods. In [11], the authors utilize Mean Field Game (MFG) and reinforcement learning for efficient beam steering among the ultra-dense beams in multi-UAV mmWave networks. However, reinforcement learning takes too much time to converge.

The work in [12] is a successful field trial of a multi-DBS MIMO network with 2×8 antennas and 3D beamforming. Because of its structure and high mobility DBSs can easily be deployed. However, its constraints about power leaves us with the problem of effective deployment of UAVs. A considerable amount of effort has been devoted to the deployment of DBS-assisted network infrastructures. In [13] authors handle the UAV deployment issue in two stages. First, they derive the downlink coverage probability for a UAV and then they propose an efficient deployment method by using circle packet theory. In [14] authors convert deployment problem into Mixed Integer Non-Linear Problem (MINLP) and solve it by using a combination of the interior point optimizer of MOSEK and bisection search. In [4] authors address the DBS deployment problem in order to maximize the sum of logarithm of achievable rates of users, which provides proportional fairness. To solve this problem, they use K-means clustering to group users and propose a Particle Swarm Optimization (PSO) algorithm. In [15], the deployment problem is formulated as two models which are the optimal coverage problem and the optimal connectivity problem. In the scope of the optimal coverage problem PSO is presented as a solution. For optimal connectivity authors propose the local network generation algorithm. In [16] the authors formulate the problem in 2D and they aim to maximize the number of users with guaranteed data rates. In [17] authors handle the UAV deployment problem from a total cost perspective. They divide total cost in the fixed cost which depends on the number of DBSs and operation cost which depends on energy consumed by UAV. Also they divide operation cost in two as power needed by the UAV to hover and power consumed in signal transmission. They search for a balance between these two types of cost and propose a solution using PSO. However, none of this work considers the mmWave band and MIMO beamforming. The authors in [18] consider 3D placement of a single DBS in order to maximize the coverage in the presence of random human blockers. However, in [18] the MIMO beamforming problem is not addressed. In [19] the authors use stochastic geometry tools in order to analyze the LoS probability, interference and achievable capacity in order to find the optimal altitude of the DBSs. The work in [20] aims to provide LoS coverage to all ground users by adjusting the orientation of the DBS antenna array. This work does not address the problem of MIMO beamforming. In [6] the authors consider a system with a single DBS and they utilize approximate beam patterns to simplify the beamforming problem. They use meta-heuristic methods and an exhaustive search to solve the joint problem of deployment and beamforming. Hence, in a great majority of the

work a single DBS is deployed and the joint problem of beamforming and DBS deployment is not addressed.

1.3 Our contribution

In this work our contribution is that: 1) we consider the deployment of multiple drone base stations; 2) we assume that each drone has a planar array of antennas, which can serve multiple ground users simultaneously; 3) we address the problem of drone base station deployment and propose two alternative solutions, such as a meta-heuristic and a heuristic algorithm; 4) we take an optimization approach for the analog beamforming, and propose a semi-definite programming-based solution. We also propose a much simpler algorithm based on Discrete Fourier Transform (DFT)-based precoding vectors. This work is an extension of the work in [21]. The current work extends the previous work [21] in many ways, such as: 1) improvement of DFT-based precoding algorithm for a better performance; 2) implementation of the particle swarm optimization algorithm for DBS deployment, as the near-optimal benchmark; 3) targeting proportional fairness as the performance objective.

The remainder of this paper is organized as follows. A system model for multiple UAVs, computational 3D mmWave channel model and problem formulation are explained in Section 2. In Section 3 beamforming techniques and complexity issues are addressed. In Section 4 DBS positioning methods and user association are presented. Numerical results are analyzed in Section 5. Finally, conclusions are given in Section 6.

2. SYSTEM MODEL

We assume that there are a number of ground users that are uniformly randomly distributed on the coverage area. Let $(x_i, y_i, 0)$ be the coordinate of user $i \in \mathcal{K}$. Each user has a single antenna. There are a set of U Drone Base Stations (DBSs), where (x_u, y_u, h_u) is the 3D coordinate of drone u . We assume quadrotor DBSs, which can hover at a fixed coordinate and assumed to maintain a fixed attitude. We assume that the exact locations of the ground users are known by the DBSs. Each drone has a panel antenna that is directed perpendicularly to the coverage area. Let $C_u = (x_u, y_u, h_u)$ be the 3D coordinate of the DBS u . Let $D_{i,u} = \sqrt{(x_i - x_u)^2 + (y_i - y_u)^2}$ be the horizontal distance of user i from the DBS u . Let $\eta_{i,u} = \arctan(\frac{h_u}{D_{i,u}})$ be the elevation angle of user i with respect to DBS u in degrees. Let $d_{i,u} = \sqrt{h_u^2 + D_{i,u}^2}$ be the actual 3D distance from DBS u to user i . A drone antenna is an array of dimensions $N \times N$. We assume that the spacing between rows and columns is half wavelength. Let P be the transmit power of each of the RF chains of the DBSs. Analog beamforming is implemented at the drone, based on the channel feedback. Let $\mathbf{w}_{i,u} = [w_{i,u,1}, w_{i,u,2}, \dots, w_{i,u,N^2}] \in \mathbb{C}^{N^2}$ be the $N^2 \times 1$ beam-

forming vector from DBS u to user i . Each element of the vector $\mathbf{w}_{i,u}$ is enforced to have the same absolute value, which is $|w_{i,u,n}| = \frac{1}{N}, \forall n = 1, \dots, N^2$. This is called the constant modulus constraint. We assume that each DBS antenna has $K_{max} \ll N^2$ RF chains, therefore K_{max} users can be served simultaneously. Once deployed, a DBS is assumed to stay fixed. Hovering inaccuracy [22] due to the rotational motion of the drones is neglected and beyond the scope of this work.

2.1 Channel model

A channel model consists of path loss and multipath components.

2.1.1 Path loss

Path loss largely depends on whether the user is obstructed by the surrounding buildings, or not. A user is in Line-of-Sight (LoS) or non-Line-of-Sight (nLoS) probabilistically depending on its elevation angle. The probability of being in LoS is as follows, [23],

$$p_{LoS,i}(\eta_{i,u}) = \frac{1}{1 + a \exp(-b(\eta_{i,u} - a))} \quad (1)$$

Here a and b are model parameters that are found experimentally in [23]. Path loss for the cases of LoS and nLoS are given in the below equation,

$$g_{i,u}(d_{i,u}, \eta_{i,u}) = \begin{cases} \left(\frac{c}{4\pi f_c}\right)^2 (d_{i,u})^{-\alpha} & nLoS \\ \left(\frac{c}{4\pi f_c}\right)^2 (d_{i,u})^{-\beta} & LoS \end{cases} \quad (2)$$

where α β are the path loss exponents ($\alpha > \beta$) for the nLoS and LoS cases, respectively.

We also have to take into account that the antennas have a pattern and limited beamwidth. The following antenna pattern is adopted, based on the 3GPP standard. [24]

$$G(90^\circ - \eta_{i,u})_{dB} = -\min \left[12 \left(\frac{90^\circ - \eta_{i,u}}{70^\circ} \right), 20 \right] \quad (3)$$

Here, 3dB beamwidth is assumed as 70 degrees and the maximum attenuation is 20 dB. $G(90^\circ - \eta_{i,u})$ is multiplied with the path loss in order to reflect the difference between the direction of interest and the boresight of the DBS antenna panel.

2.1.2 Multipath fading

MmWave channels are sparse both in the angle and delay domains. This property is experimentally verified in previous studies such as [25]. This is caused by the small number of scattering clusters and narrow angular spreads. For the multipath model we assume a flat

mmWave sparse channel model that has a limited number of multipath components. Let $\mathbf{h}_{i,u}$ be the $N^2 \times 1$ channel vector of node i from DBS u .

$$\mathbf{h}_{i,u} = \sum_{l=1}^{L_{i,u}} \lambda_{i,u,l} \mathbf{a}(N, N, \theta_{i,u,l}, \phi_{i,u,l}) \quad (4)$$

where $L_{i,u}$ is the number of paths for node i . Let $\lambda_{i,u,l}$ be the channel coefficient of path l from DBS u to node i , which is a complex Gaussian. Angles $\theta_{i,u,l}$ and $\phi_{i,u,l}$ denote the azimuth and elevation Angle of Departure (AoD) of the l^{th} path from the DBS u . Finally, $\mathbf{a}(N, N, \theta_{i,u,l}, \phi_{i,u,l})$ denotes the steering vector,

$$\begin{aligned} \mathbf{a}(N, N, \theta_{i,u,l}, \phi_{i,u,l}) &= [1, \dots, e^{j\pi \sin \theta_{i,u,l} [(n_1-1) \cos \phi_{i,u,l} + (n_2-1) \sin \phi_{i,u,l}]} \\ &\quad, \dots, e^{j\pi \sin \theta_{i,u,l} [(N-1) \cos \phi_{i,u,l} + (N-1) \sin \phi_{i,u,l}]}] \end{aligned} \quad (5)$$

We assume that out of L_i paths, the first one can be either LoS or nLoS, whereas the other paths are definitely nLoS [6]. That is the channel coefficients are,

$$\lambda_{i,u,l} = \frac{\sigma_f}{\left(\frac{4\pi f}{c}\right) d_i^\beta}, l = 2, \dots, L_i \quad (6)$$

Here σ_f is a complex Gaussian random variable, f is the carrier frequency, c is the speed of light, β is the nLoS path loss exponent. The first path can be either LoS or nLoS,

$$\lambda_{i,u,1} = \begin{cases} \frac{\sigma_f}{\left(\frac{4\pi f}{c}\right) d_{i,u}^{\beta/2}} & nLoS \\ \frac{\sigma_f}{\left(\frac{4\pi f}{c}\right) d_{i,u}^{\alpha/2}} & LoS \end{cases} \quad (7)$$

where α is the LoS pathloss exponent. Typically α and β are 0.95 and 1.65, respectively.

We assume that the transmitters have the channel state information.

2.2 Problem formulation

Let u_i denote the DBS associated with ground user i . The Signal to Interference plus Noise Ratio (SINR) of user i is as follows.

$$SINR_i = \frac{P |\mathbf{h}_{i,u_i}^H \mathbf{w}_{i,u_i}|^2}{N_o + \sum_{k \neq i}^K P |\mathbf{h}_{i,u_k}^H \mathbf{w}_{k,u_k}|^2}, i = 1, \dots, K \quad (8)$$

An achievable rate can be defined as $R_i(\mathbf{w}_{i,u_i}) = \log_2(1 + SINR_i)$. We will define a joint DBS deployment, user association and beamforming problem, below. Our objective is to maximize the sum of logarithms of rates (proportional fairness) subject to a constraint on the number of RF chains (i.e. number of connected users) of each DBS. Let $x_{i,u}$ be the binary connection variable, which takes value one if user i is connected to DBS u and zero, otherwise. Then u_i becomes the index of the DBS such that $x_{i,u} = 1$.

$$\max_{x_{i,u}, \mathbf{w}_{i,u_i}, C_u \forall i,u} \left\{ \sum_{i=1}^K \sum_{u=1}^U x_{i,u} \log(R_i(\mathbf{w}_{i,u_i})) \right\} \quad (9)$$

subject to,

$$|[\mathbf{w}_{i,u_i}]_n|^2 = 1, \forall n = 1, \dots, N^2, i = 1, \dots, K \quad (10)$$

$$\sum_{i=1}^K x_{i,u} \leq K_{max}, \forall u = 1, \dots, U \quad (11)$$

$$\sum_{u=1}^U x_{i,u} = 1, \forall i = 1, \dots, K \quad (12)$$

$$x_{i,u} \in \{0, 1\}, \forall i = 1, \dots, K, u = 1, \dots, U \quad (13)$$

Here the objective function aims to maximize the proportional fairness, which is a good trade-off between total throughput and max-min fairness. Constraint (10) is the constant modulus constraint. Constraint (11) limits the number of users simultaneously served by a DBS, due to limited number of RF chains. Constraint (12) enforces each user to connect to a single DBS. Finally, Constraint (13) enforces the $x_{i,u}$ to be a binary variable. This optimization problem is a Mixed Integer Nonlinear Programming (MINLP) problem, due to the SINR expression in (8) that depends on DBS deployment locations and the logarithmic rate and objective functions, along with the binary variable $x_{i,u}$. Finding a globally optimal solution is prohibitively complex. Therefore, we will divide the problem into two such as 1) DBS deployment (determining the 3D coordinates and user-DBS associations), 2) beamforming for each DBS.

3. BEAMFORMING

Here, we will consider the problem of analog beamforming at each DBS, given the channel conditions (i.e. DBS coordinates) and the DBS-user association. Maximizing the total rate (or log sum rate) in the presence of interference is a challenging non-convex optimization problem [26]. The reason is the interference at the denominator of the SINR expression (i.e. interference leakage). An alternative is the zero forcing precoding that enforces $\mathbf{h}_{k,u_k}^H \mathbf{w}_{k,u_k} = 0, \forall i = 1, \dots, K, k \neq i$. However, enforcing zero interference may not be optimal in terms of beamforming gain and throughput. In [26] a method that jointly maximizes beamforming gain and minimizes interference leakage, is proposed. This method only depends on the Angles of Departure (AoDs) and the corresponding array steering vectors of the dominant (LoS) path from a base station to each of its users. In the DBS channel model, the first (i.e. LoS) path is significantly stronger than the others. Therefore, we only take the steering vector of the first path and define the following. Let the i th ground users $i = 1, \dots, K_u$ be connected to the DBS u . We form the following matrix by collecting the dominant path vectors for all users connected to DBS u , except the user i ,

$$\tilde{\mathbf{I}}_{i,u} = [\mathbf{a}(\theta_{1,u,1}, \phi_{1,u,1}), \dots, \mathbf{a}(\theta_{i-1,u,1}, \phi_{i-1,u,1}), \mathbf{a}(\theta_{i+1,u,1}, \phi_{i+1,u,1}), \dots, \mathbf{a}(\theta_{K_u,u,1}, \phi_{K_u,u,1})] \quad (14)$$

Singular Value Decomposition (SVD) is performed in order to find the null space of $\tilde{\mathbf{I}}_{i,u}$,

$$\tilde{\mathbf{I}}_{i,u} = \tilde{\mathbf{U}}_{i,u} \tilde{\mathbf{\Sigma}}_{i,u} [\tilde{\mathbf{V}}_{i,u}^{(1)} \tilde{\mathbf{V}}_{i,u}^{(0)}] \quad (15)$$

$\tilde{\mathbf{V}}_{i,u}^{(1)}$ holds the first $K_{max} - 1$ right singular vectors and $\tilde{\mathbf{V}}_{i,u}^{(0)}$ holds the $N^2 - K_{max} + 1$ right singular vectors. There are two objectives. The first objective, minimizing the leakage interference, is equivalent to maximizing the projection of $\mathbf{w}_{i,u}$ on the null space $\tilde{\mathbf{V}}_{i,u}^{(0)}$. The second objective, maximizing the beamforming gain is equivalent to maximizing $\mathbf{w}_{i,u}^H \mathbf{a}(\theta_{i-1,u,1}, \phi_{i-1,u,1}) \mathbf{a}(\theta_{i-1,u,1}, \phi_{i-1,u,1})^H \mathbf{w}_{i,u}$. The two objectives are combined in a weighted manner where the leakage and gain objectives are multiplied with weights λ_1 and λ_2 , where $\lambda_1 + \lambda_2 = 1$. The problem becomes convex by converting it into Semi-Definite Programming (SDP). First, let us define $\mathbf{W} = \mathbf{w}_{i,u} \mathbf{w}_{i,u}^H$, which is a square, symmetric semi-definite matrix. The optimization problem becomes,

$$\max_{\mathbf{W}} Tr((\lambda_1 \tilde{\mathbf{V}}_{i,u}^{(0)} (\tilde{\mathbf{V}}_{i,u}^{(0)})^H + \lambda_2 \mathbf{a}(\theta_{i-1,u,1}, \phi_{i-1,u,1}) \mathbf{a}(\theta_{i-1,u,1}, \phi_{i-1,u,1})^H) \mathbf{W}) \quad (16)$$

such that,

$$[\mathbf{W}]_{i,i} = \frac{1}{N^2} \quad (17)$$

$$\mathbf{W} \succeq 0 \quad (18)$$

$$Rank(\mathbf{W}) = 1 \quad (19)$$

The last (Rank 1) constraint can be relaxed, which makes the problem convex. This is called semi-definite relaxation. Then the problem can be solved using off-the-shelf programs such as *cvx*. Then, using the resulting optimal \mathbf{W} , the precoding vector $\mathbf{w}_{i,u}$ can be found using Gaussian randomization.

3.1 Oversampled DFT-based codebook

In 5G New Radio (5G NR), Type-I precoding utilizes oversampled DFT-based codebooks for precoding [27]. For a Uniform Linear Array (ULA) of length N , the DFT precoder is,

$$\mathbf{w}_{1D}(k) = [e^{j2\pi \cdot 0 \cdot \frac{k}{ON}}, e^{j2\pi \cdot 1 \cdot \frac{k}{ON}}, \dots, e^{j2\pi \cdot (N-1) \cdot \frac{k}{ON}}]^T, k = 0, 1, \dots, ON - 1 \quad (20)$$

Here O is the integer oversampling factor, which is typically taken as $O = 4$. A set of precoders for a 2D array, e.g. Uniform Planar Array (UPA), can be obtained taking the

Kronecker product $w_{2D}(k, l) = w_{1D}(k) \otimes w_{1D}(l)$. This precoder can be extended for dual polarization, however we assume single polarization in this work. As a result, for an $N \times N$ array and $O = 4$ oversampling factor there is a total of $N^2 O^2$ alternatives for a precoding vector. This is a type of quantization in the angular domain and significantly reduces the required CSI feedback overhead. In the LTE implementation, each ground user feeds back its optimal precoding vector, without taking into account interference from users attached to the same DBS and other DBSs.

Let $\mathcal{V} = [\mathbf{w}_{2D}(1), \dots, \mathbf{w}_{2D}(v), \dots, \mathbf{w}_{2D}(O^2 N^2)]$ be the set of precoding vectors produced according to ((20)). Let v_i be the index of the vector chosen for user i .

$$v_i = \arg \max_{v \in \mathcal{V}} \frac{|\mathbf{h}_{i,u_i}^H \mathbf{w}_{2D}(v)|^2}{\sum_{k \neq i} |\mathbf{h}_{k,u_i}^H \mathbf{w}_{2D}(v)|^2}, i = 1, \dots, K \quad (21)$$

This is the ratio of gain of user i to the interference leakage that is created to all other users. This method requires the DBS-user associations and channel conditions as the input.

3.2 Complexity issues

The SDP-based solution consists of an interior point method to solve the relaxed SDP problem and the randomized algorithm in order to find a rank-one solution. A Gaussian randomization algorithm consists of repeated applications of Cholesky factorization. A solution of SDP using interior point methods has a complexity of $O((N^2)^3)$ [28], which is the cubic of number of antenna elements. Cholesky factorization has also a similar complexity. Therefore, the complexity is roughly in cubics of the number of antenna elements. On the other hand, a codebook-based method chooses the optimal precoding vector among $O(N^2)$ alternatives; therefore it has $O(N^2)$ complexity.

4. DBS POSITIONING AND USER ASSOCIATION

Let \mathcal{K}_u be the set of users associated with DBS u . In this work we assume that $K = K_{max} \times U$, and each DBS will be associated with exactly K_{max} users in order to serve all users¹.

4.1 K-means clustering

Having the channel state information to a ground user from every point in the 3 dimensional space is not feasible. Therefore, horizontal DBS positioning and user-DBS association is performed only based on the location of

the ground users. K-means clustering is an effective tool to group geographically close users, where a DBS is deployed at the centroid of each cluster of ground users [4]. Each DBS is located at the center of its cluster of ground users. However, unlike the regular K-means algorithm, in the current scenario each cluster has to have a size limit of K_{max} ground users [29]. We describe the K-means-1 algorithm in the pseudocode 1.

Algorithm 1 K-means-1 Algorithm

- 1: Initialize cluster centroids $(x_u, y_u), \forall u \in \mathcal{U}$
 - 2: **while** not converge **do**
 - 3: $\mathcal{A} = \mathcal{U}, m_i = 0, u_i = 0, \forall i \in \mathcal{K}$
 - 4: Calculate $D_{i,u} = \sqrt{(x_i - x_u)^2 + (y_i - y_u)^2}, \forall i \in \mathcal{K}, u \in \mathcal{U}$
 - 5: sort $D_{i,u}, \forall i \in \mathcal{K}$ in ascending order
 - 6: $m_i = D_{i,u^{(1)}} - D_{i,u^{(2)}}, \forall i \in \mathcal{K}$
 - 7: Sort m_i in descending order
 - 8: **for** $k = 1 : K$ **do**
 - 9: $u^* = \min_{u \in \mathcal{A}} \{D_{i^{(k)},u}\}$
 - 10: $u_{i^{(k)}} = u^*$
 - 11: **if** $|i : \exists i \text{ s.t. } u_i = u^*| = K_{max}$ **then**
 - 12: $\mathcal{A} = \mathcal{A}/u^*$
 - 13: **end if**
 - 14: **end for**
 - 15: Update 2D DBS coordinates $(x_u, y_u) \leftarrow \frac{1}{K_{max}} \sum_{i \text{ s.t. } u_i = u} (x_i, y_i), \forall u \in \mathcal{U}$
 - 16: **end while**
 - 17: Find $\arg \max_{h_u} \{C_u(h_u)\}, \forall u \in \mathcal{U}$ ((22))
 - 18: Return $(x_u, y_u, h_u), \forall u \in \mathcal{U}$
-

Line 1 initializes the cluster centroids. This can be done by randomly choosing distinct ground user locations as the centroids. The main loop of clustering are lines 2-16. Each loop starts by initializing the available DBSs as \mathcal{U} and resetting the metrics and connections (Line 3). User-DBS distances are updated in line 4 (Complexity $O(KU)$). For each user line 5 sorts the 2D DBS distances in ascending order and metric for each user is calculated as the difference of the first and second element of the sorted array (line 6) (Complexity $O(KU)$). This reflects the opportunity cost of not assigning a user to its closest DBS. Line 7 sorts the user metrics in descending order (Complexity $O(K \log_2(K))$). The for loop in lines 8 to 14 goes over the users in descending order of metric and assigns the best available DBS (Complexity $O(KU)$). A DBS ceases to be available once K_{max} users are connected to it. The while loop is repeated until a convergence criterion is met. The overall complexity of the K-means-1 algorithm is $O(KU + K \log_2 K)$.

Pseudocode 2 shows the K-means-2 algorithm. The difference of K-means-2 from the first version is that it updates the user metrics after each user-DBS association. The reason is that once a DBS is not available, there is no point in taking it into account in calculating the user metrics. However it has higher complexity, which is roughly

¹The case of $K > K_{max} \times U$ requires scheduling and time sharing among groups of users, which is a case of future study.

$O(UK \log_2(K))$.

Algorithm 2 K-means-2 Algorithm

```

1: Initialize cluster centroids  $(x_u, y_u), \forall u \in \mathcal{U}$ 
2: while not converge do
3:    $\mathcal{A} = \mathcal{U}, \mathcal{F} = \mathcal{K}, m_i = 0, u_i = 0, \forall i \in \mathcal{K}$ 
4:   for  $k = 1 : K$  do
5:     Calculate  $D_{i,u} = \frac{1}{\sqrt{(x_i - x_u)^2 + (y_i - y_u)^2}}, \forall i \in \mathcal{F}, u \in \mathcal{A}$ 
6:     sort  $D_{i,u}, \forall i \in \mathcal{F}, u \in \mathcal{A}$  in ascending order
7:      $m_i = D_{i,u^{(1)}} - D_{i,u^{(2)}}, \forall i \in \mathcal{F}$ 
8:      $i^* = \max_{i \in \mathcal{F}} \{m_i\}$ 
9:      $u^* = \min_{u \in \mathcal{A}} \{D_{i^*,u}\}$ 
10:     $u_{i^*} = u^*$ 
11:    if  $|i : \exists i \text{ s.t. } u_i = u^*| = K_{max}$  then
12:       $\mathcal{A} = \mathcal{A}/u^*$ 
13:    end if
14:  end for
15:  Update 2D DBS coordinates  $(x_u, y_u) \leftarrow \frac{1}{K_{max}} \sum_{i \text{ s.t. } u_i = u} (x_i, y_i), \forall u \in \mathcal{U}$ 
16: end while
17: Find  $\arg \max_{h_u} \{C_u(h_u)\}, \forall u \in \mathcal{U}$  ((22))
18: Return  $(x_u, y_u, h_u), \forall u \in \mathcal{Y}$ 
    
```

After the 2D (horizontal) DBS coordinates and user-DBS association is determined, both algorithms K-means-1 and K-means-2 adjust the height of each base station. The objective is,

$$C_u(h_u) = \sum_{i \text{ s.t. } u_i = u} \log(R'_i(h_{u_i})) \quad (22)$$

This objective reflects sum of logarithms of rates of users connected to a DBS. ($R'_i(h_{u_i})$ is the rate expression used in this objective function. It is defined as in Equation (23), which is taken from [30] and [31].

4.2 Particle swarm optimization

Finding the optimal locations of multiple base stations is a nonlinear and non-convex problem. Particle Swarm Optimization (PSO) [32] has been proven as a good candidate to solve nonlinear continuous optimization problems. In this method candidate solutions, denoted as *particles* are randomly generated. Each particle has a *fitness*, which is a measure of its performance. The particle values are iteratively updated based on their fitness and its personal best fitness, as well as the global best fitness of all particles. The pseudocode of the PSO algorithm is shown in Algorithm 3.

There are N_p particles and they are randomly initialized in line 1 of the algorithm. Each particle contains $3K \times 1$ numbers, which are the 3D coordinates of the DBSs. The global best particle and its fitness, along with the personal best value and fitness of each particle are initialized in line 2. Line 5 calculates a rate expression for each DBS-user pair according to ((23)). The for loop in lines 7-16,

similar to the K-means algorithm, assigns users to DBSs. The difference is the metric, which is based on the rate instead of distance. Line 18 calculates the fitness for each particle. In lines 19-24 personal and global best particles and their fitnesses are updated. Finally Line 26 updates the particle positions. Learning coefficients c_0, c_1 and c_2 are determined according to [32].

Algorithm 3 PSO Algorithm

```

1: Initialize random particles  $p^p = (x_u^p, y_u^p, h_u^p), \forall u \in \mathcal{U}, p = 1, \dots, N_p$ 
2: Initialize  $gbest_f, lbest_f^p, lbest^p, \forall p = 1, \dots, N_p$ 
3: while not converge do
4:   for  $p = 1 : N_p$  do
5:     Calculate  $R'_i(x_u^p, y_u^p, h_u^p), \forall i \in \mathcal{K}, u \in \mathcal{U}$ 
6:      $\mathcal{A} = \mathcal{U}, \mathcal{F} = \mathcal{K}, m_i = 0, u_i = 0, \forall i \in \mathcal{K}$ 
7:     for  $k = 1 : K$  do
8:       Calculate  $R'_i(x_u^p, y_u^p, h_u^p), \forall i \in \mathcal{K}, u \in \mathcal{U}$ 
9:       sort  $R'_i(x_u^p, y_u^p, h_u^p), \forall i \in \mathcal{F}, u \in \mathcal{A}$  in ascending order
10:       $m_i = R'_i(x_u^p, y_u^p, h_u^p) - R'_i(x_u^p, y_u^p, h_u^p), \forall i \in \mathcal{F}$ 
11:       $i^* = \max_{i \in \mathcal{F}} \{m_i\}$ 
12:       $u^* = \min_{u \in \mathcal{A}} \{D_{i^*,u}\}$ 
13:       $u_{i^*}^p = u^*$ 
14:      if  $|i : \exists i \text{ s.t. } u_i = u^*| = K_{max}$  then
15:         $\mathcal{A} = \mathcal{A}/u^*$ 
16:      end if
17:    end for
18:     $f^p = \sum_{i \in \mathcal{K}} \log(R'_i(x_{u_i}^p, y_{u_i}^p, h_{u_i}^p)), \forall p = 1, \dots, N_p$ 
19:    if  $f^p > lbest_f^p$  then
20:      Update local best:  $lbest_f^p = f^p, lbest^p = (x_u^p, y_u^p, h_u^p)$ 
21:    end if
22:    if  $f^p > gbest_f$  then
23:      Update global best:  $gbest_f = f^p, gbest^p = (x_u^p, y_u^p, h_u^p)$ 
24:    end if
25:  end for
26:  Update particles  $p^{p+} = c_0 \times \text{rand} + c_1 \times (lbest^p - p^p) + c_2 \times (gbest - p^p)$ 
27: end while
    
```

5. NUMERICAL RESULTS

In this section, we will compare the performances of 5 schemes:

- PSO + SDP: Uses particle swarm optimization for the DBS deployment and SDP for the precoding optimization.
- K-means-1+SDP: Uses Option 1 in K-means clustering and SDP-based precoding optimization.
- K-means-2+SDP: Uses Option 2 in K-means clustering and SDP-based precoding optimization.

$$R'_i(h_{u_i}) = p_{LoS,i}(\eta_{i,u}) \log_2 \left(1 + \frac{N^2 - K_{max} + 1}{K_{max}} \frac{Pg_{i,u_i}^{LoS}(d_{i,u_i}, \eta_{i,u_i})}{N_o} \right) + p_{NLoS,i}(\eta_{i,u}) \log_2 \left(1 + \frac{N^2 - K_{max} + 1}{K_{max}} \frac{Pg_{i,u_i}^{NLoS}(d_{i,u_i}, \eta_{i,u_i})}{N_o} \right) \quad (23)$$

- K-means-1+DFT: Uses Option 1 in K-means clustering and DFT-based precoding codebook.
- K-means-2+DFT: Uses Option 2 in K-means clustering and DFT-based precoding codebook.

24 ground users are randomly located in a circular area of radius of 1000 meters. The carrier frequency is 28 GHz. There are $K = 4$ DBSs, where each DBS has a uniform panel antenna with 8×8 elements (unless otherwise stated) with half wavelength spacing. Each DBS has $K_{max} = 6$ RF chains. The transmit power per RF chain is 10 Watts and noise power is $N_o = 1 \times 10^{-13}$ Watt. LoS probability parameters are $a = 11.95$ and $b = 0.14$, respectively (i.e. "Urban" scenario). The channel from each DBS to each ground user has $L_i = 4$ paths. Each point on a graph is the average of 100 independent runs.

In Fig. 1 we evaluate the effects of changing λ_2 (hence λ_1) on the throughput performance. Parameters λ_1 and $\lambda_2 = 1 - \lambda_1$ are the weights of interference and beamforming gain, respectively. All simulations are done for $K = 24$ users distributed on a circular area of radius 1000 meters. There are 3 subplots, which are for different configurations, namely $U = 4, K_{max} = 6, U = 6, K_{max} = 4$ and $U = 8, K_{max} = 3$. Results reveal that λ_2 should be small for optimal performance. This is because λ_2 is the weight of beamforming gain for the transmitted user (which is supposed to be high), while λ_1 is the weight of projection on null-space (i.e. interference leakage), which is supposed to be small. Results show that $\lambda_2 = 0.001$ (i.e. $\lambda_1 = 0.999$) is a good choice. As the number of DBSs is increased, optimal λ_2 gets smaller. The reason is that when there are more DBSs, each covers less users. Therefore, they can decrease their altitude, which decreases the inter-DBS interference, hence its weight (λ_1) should be higher.

Table 1 shows the average total, minimum and log-sum average throughput performance of the five schemes, which are compared with respect to different numbers of DBSs and RF chains. The number of DBSs are taken as $U = 4, 6$ and 8 . The product of the number of DBSs and RF chains are kept fixed at 24, which is the number of users. The minimum rate is a metric for fairness and log-sum throughput is a metric of proportional fairness, which is a trade-off between throughput and fairness. λ_1 is taken as 0.999. Results reveal that as the number of DBSs increases, the performance gets better. This is an expected result, because, as the number of

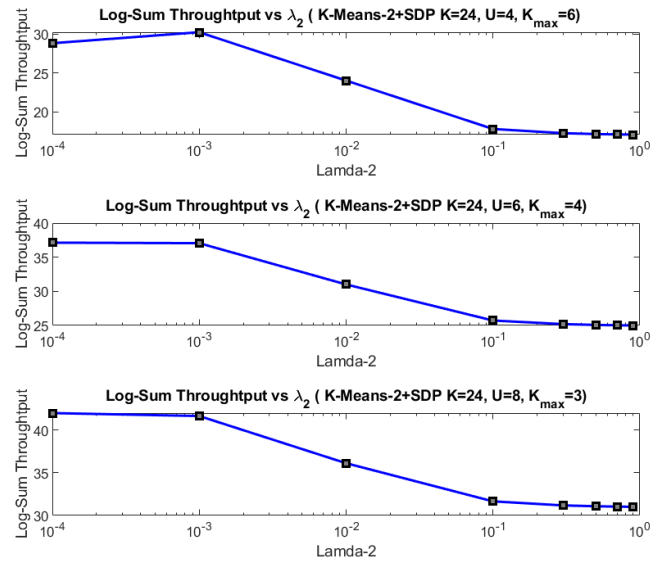


Fig. 1 – Log-sum throughput vs. λ_2 (interference weight). The throughput makes a peak, if λ_1 is close to one (i.e. λ_2 is close to zero.)

DBSs are increased, each DBS has to cover less number of users. The DBS height can be decreased and the path loss decreases. Results also reveal that the clustering algorithms K-means-1 and 2 have similar performances in terms of log-sum throughput. For fewer DBSs, K-means-2 is slightly better, while for 8 DBSs K-means-1 is better. Considering the complexity of both algorithms and their performance, K-means-1 is more preferable.

A comparison between K-means and PSO shows that PSO is 10% better in terms of throughput and proportional fairness, for 4 DBSs. PSO requires significantly more time to converge. Besides, it requires centralized implementation. Considering these disadvantages, we can say that K-means strikes a good balance between performance and complexity.

Lastly, comparing SDP-based beamforming and DFT-based beamforming, we can observe that the difference is significant for fewer DBSs. This is because for fewer DBSs, the DBSs' heights become higher and there may be a significant amount of interference among different DBSs. An SDP-based solution better manages this interference. On the other hand, for higher number of DBSs, interference is less of a problem and the performance gap between the SDP and DFT-based methods decreases.

Figures 2, 3 and 4 show the logarithmic sum of

Table 1 – Different configurations and performance criteria (24 users)

Configuration	Total throughput (bps/Hz)		
	$U = 4, K_{max} = 6$	$U = 6, K_{max} = 3$	$U = 8, K_{max} = 3$
K-means-1+SDP	128.91	154.83	177.47
K-means-2+SDP	129.78	155.14	173.64
K-means-1+DFT	99.20	130.95	158.05
K-means-2+DFT	100.55	132.03	155.11
PSO+SDP	139.32	166.84	192.81
Configuration	Minimum throughput(bps/Hz)		
	$U = 4, K_{max} = 6$	$U = 6, K_{max} = 3$	$U = 8, K_{max} = 3$
K-means-1+SDP	0.27	0.72	1.04
K-means-2+SDP	0.46	0.72	0.99
K-means-1+DFT	0.14	0.38	0.64
K-means-2+DFT	0.17	0.38	0.63
PSO+SDP	0.67	1.01	1.56
Configuration	Log-sum throughput (proportional fairness)		
	$U = 4, K_{max} = 6$	$U = 6, K_{max} = 3$	$U = 8, K_{max} = 3$
K-means-1+SDP	30.09	37.60	42.77
K-means-2+SDP	30.26	37.05	41.65
K-means-1+DFT	23.61	33.11	39.69
K-means-2+DFT	24.08	33.16	38.94
PSO+SDP	33.76	40.36	45.72

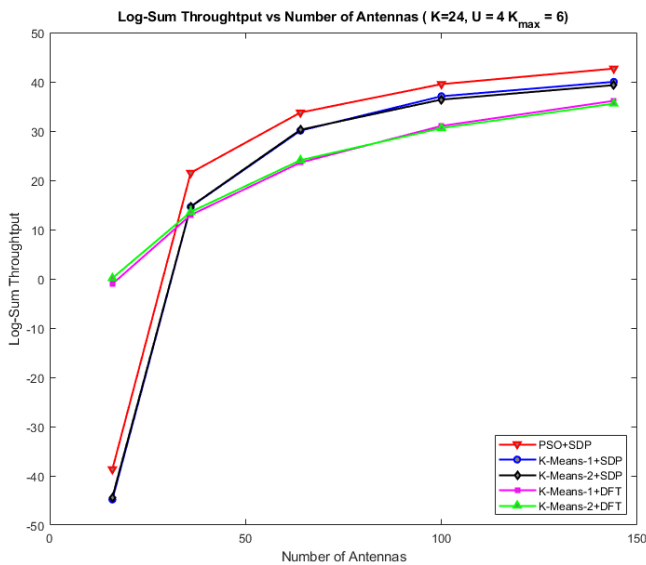


Fig. 2 – Log-sum throughput vs. number of antennas for $U = 4$ DBSs and $K_{max} = 6$ RF chains per DBS

achievable user throughput versus the number of antenna elements at the DBS. Simulations are run for $\lambda = 0.999$. The observations are as follows:

- First of all, as the number of DBSs is increased, log-sum throughput increases, which is expected.
- Secondly, the three figures reveal that the variations on the K-means algorithm has a negligible effect on

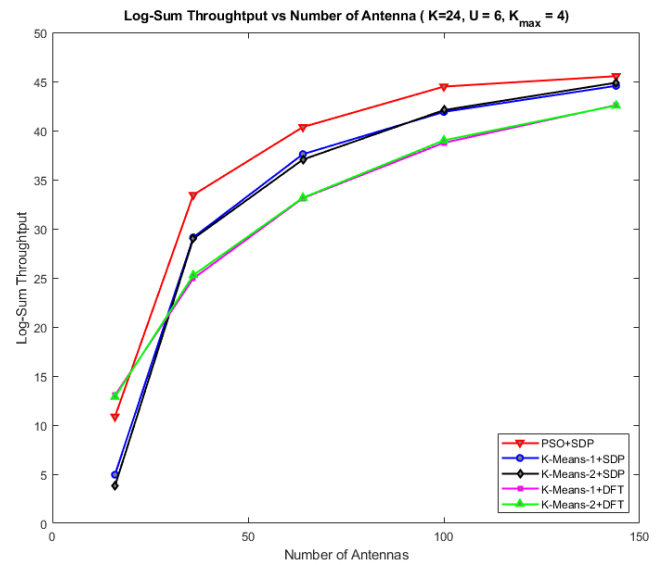


Fig. 3 – Log-sum throughput vs. number of antennas for $U = 6$ DBSs and $K_{max} = 4$ RF chains per DBS

the performance.

- Log-sum throughput is an increasing concave function of number of antennas. Increasing the number of antennas provides diminishing returns.
- For $U = 4, 6, 8$ DBSs, the percentage difference between the SDP and DFT decreases as the number of antennas is increased. DFT performs within 5% of SDP for $U = 6$ or $U = 8$ DBSs and $N^2 = 144$

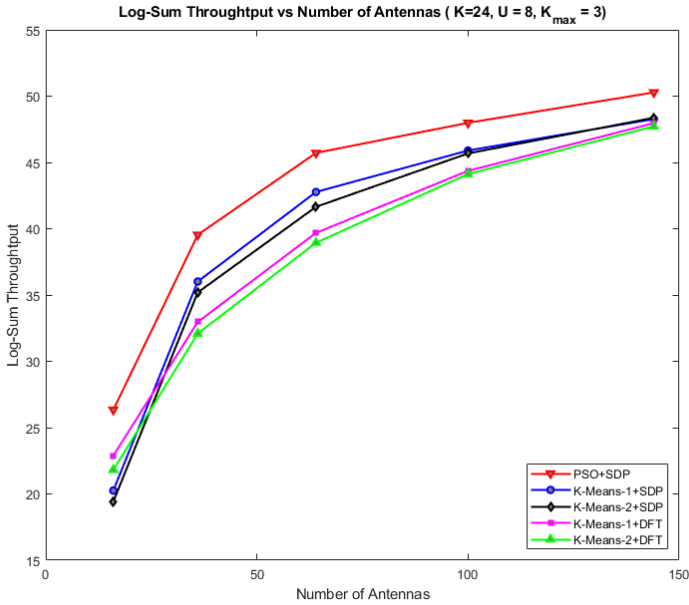


Fig. 4 – Log-sum throughput vs. number of antennas for $U = 8$ DBSs and $K_{max} = 3$ RF chains per DBS

antenna elements. This shows the effectiveness of using a simple DFT-based codebook.

- The percentage difference between the PSO and K-means-based DBS deployment schemes decrease as the number of antennas is increased.
- Interestingly, for $U = 4$ and 6 DBSs and a very small number of antennas (e.g. $N^2 = 16$), a DFT-based beamforming scheme performs better than SDP-based beamforming. Please note that, this is a poor performance of SDP, rather than a good performance of DFT. Especially for $U = 4$ we observe a negative log-sum throughput. This points to a close-to-zero throughput for at least one user for most of the trials. The reason is as follows: For $N^2 = 16$ antennas, the degree of freedom (e.g. the null space) is smaller. Then, the SDP method fails in finding beamforming vectors that have good projection on the null space. SDP is clearly performing well for $N^2 > K$

In Fig. 5 empirical cumulative distribution of user SINRs (in dB) are plotted for various methods. The results reveal that the K-means algorithm performs quite close to the PSO-based near-optimal benchmark. However, the difference between the SDP-based beamforming and DFT codebooks is more significant. For example, the probability of SNR being smaller than 0 dB is 0.1 for DFT, while it is around 0.05 for the SDP. Finally, the performance difference between two variations of K-means clustering is negligible.

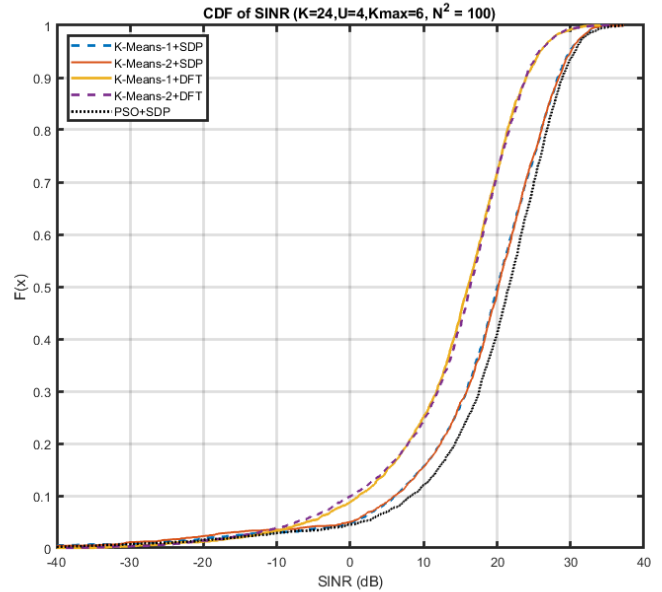


Fig. 5 – Empirical cumulative distribution of user SINR values for $N^2 = 100$ antennas, $U = 4$ DBSs and $K_{max} = 6$ RF chains per DBS

6. CONCLUSIONS

In this work we studied the problem of deploying multiple mmWave Drone Base Stations (DBS) that perform MIMO analog beamforming in order to efficiently serve a number of ground users. K-means clustering and height adjustment is shown to be a promising method in order to deploy DBSs and associate users to them. However, cluster size constraints (due to a limited number of RF chains) requires clever application of the algorithm. The proposed method performs close to a benchmark that is based on Particle Swarm Optimization (PSO). On the other hand, using a simple DFT-based codebook performs quite close to a Semi-Definite Programming (SDP)-based optimal beamforming, especially for large number of antennas.

In reality, the number of ground users may be way more than the total number of RF chains. This requires further grouping and scheduling of users in time, which is a subject of future work. Secondly, the considered SDP-based method only minimizes the interference from the ground users that are attached to the same DBS. Methods to address interference from other DBSs need to be investigated. Moreover, methods to optimize DBS power also need to be researched. Other topics to be investigated involve different and more realistic channel models, channel estimation issues, beam training, and individual rate constraints.

REFERENCES

- [1] A. Abdelkefi M. Hassanalian. "Classifications, applications, and design challenges of drones: A review". In: *Progress in Aerospace Sciences 91* (2017), pp. 99–131.
- [2] Ahmet Yazar, S Dogan-Tusha, and Huseyin Arslan. "6G vision: An ultra-flexible perspective". In: *ITU Journal on Future and Evolving Technologies 1.1* (2020), pp. 121–140.
- [3] Sara Garcia Sanchez, Subhramoy Mohanti, Dheryta Jaisinghani, and Kaushik Roy Chowdhury. "Millimeter-wave base stations in the sky: An experimental study of UAV-to-ground communications". In: *IEEE Transactions on Mobile Computing* (2020).
- [4] Alper Akarsu and Tolga Girici. "Fairness aware multiple drone base station deployment". In: *IET Communications 12.4* (2018), pp. 425–431.
- [5] Chiya Zhang, Weizheng Zhang, Wei Wang, Lu Yang, and Wei Zhang. "Research challenges and opportunities of UAV millimeter-wave communications". In: *IEEE Wireless Communications 26.1* (2019), pp. 58–62.
- [6] Zhenyu Xiao, Hang Dong, Lin Bai, Dapeng Oliver Wu, and Xiang-Gen Xia. "Unmanned aerial vehicle base station (UAV-BS) deployment with millimeter-wave beamforming". In: *IEEE Internet of Things Journal 7.2* (2019), pp. 1336–1349.
- [7] Zhenyu Xiao, Pengfei Xia, and Xiang-Gen Xia. "Enabling UAV cellular with millimeter-wave communication: Potentials and approaches". In: *IEEE Communications Magazine 54.5* (2016), pp. 66–73.
- [8] Jianwei Zhao, Feifei Gao, Qihui Wu, Shi Jin, Yi Wu, and Weimin Jia. "Beam tracking for UAV mounted SatCom on-the-move with massive antenna array". In: *IEEE Journal on Selected Areas in Communications 36.2* (2018), pp. 363–375.
- [9] Lipeng Zhu, Jun Zhang, Zhenyu Xiao, Xianbin Cao, Dapeng Oliver Wu, and Xiang-Gen Xia. "3-D beamforming for flexible coverage in millimeter-wave UAV communications". In: *IEEE Wireless Communications Letters 8.3* (2019), pp. 837–840.
- [10] Hossein Vaezy, Mehdi Salehi Heydar Abad, Ozgur Ercetin, Halim Yanikomeroglu, Mohammad Javad Omidi, and Mohammad Mahdi Naghsh. "Beamforming for maximal coverage in mmWave drones: A reinforcement learning approach". In: *IEEE Communications Letters 24.5* (2020), pp. 1033–1037.
- [11] Qianqian Cheng, Lixin Li, Kaiyuan Xue, Huan Ren, Xu Li, Wei Chen, and Zhu Han. "Beam-steering optimization in multi-UAVs mmWave networks: A mean field game approach". In: *2019 11th International Conference on Wireless Communications and Signal Processing (WCSP)*. IEEE. 2019, pp. 1–5.
- [12] Yiming Huo and Xiaodai Dong. "Millimeter-wave for unmanned aerial vehicles networks: Enabling multi-beam multi-stream communications". In: *arXiv preprint arXiv:1810.06923* (2018).
- [13] Mohammad Mozaffari, Walid Saad, Mehdi Bennis, and Mérouane Debbah. "Efficient deployment of multiple unmanned aerial vehicles for optimal wireless coverage". In: *IEEE Communications Letters 20.8* (2016), pp. 1647–1650.
- [14] R Irem Bor-Yaliniz, Amr El-Keyi, and Halim Yanikomeroglu. "Efficient 3-D placement of an aerial base station in next generation cellular networks". In: *2016 IEEE international conference on communications (ICC)*. IEEE. 2016, pp. 1–5.
- [15] Xiaofei He, Wei Yu, Hansong Xu, Jie Lin, Xinyu Yang, Chao Lu, and Xinwen Fu. "Towards 3D deployment of UAV base stations in uneven terrain". In: *2018 27th International Conference on Computer Communication and Networks (ICCCN)*. IEEE. 2018, pp. 1–9.
- [16] Chuan-Chi Lai, Chun-Ting Chen, and Li-Chun Wang. "On-demand density-aware UAV base station 3D placement for arbitrarily distributed users with guaranteed data rates". In: *IEEE Wireless Communications Letters 8.3* (2019), pp. 913–916.
- [17] Achal Agrawal Bhanukiran Perabathini Kiranteya Tummuri and Vineeth S Varma. "Efficient 3D placement of UAVs with QoS assurance in ad hoc wireless networks". In: *2019 28th International Conference on Computer Communication and Networks (ICCCN)*. IEEE. 2019.
- [18] Margarita Gapeyenko, Irem Bor-Yaliniz, Sergey Andreev, Halim Yanikomeroglu, and Yevgeni Koucheryavy. "Effects of blockage in deploying mmWave drone base stations for 5G networks and beyond". In: *2018 IEEE international conference on communications workshops (icc workshops)*. IEEE. 2018, pp. 1–6.
- [19] Wenqiang Yi, Yuanwei Liu, Maged Elkashlan, and Arumugam Nallanathan. "Modeling and coverage analysis of downlink UAV networks with mmWave communications". In: *2019 IEEE International Conference on Communications Workshops (ICC Workshops)*. IEEE. 2019, pp. 1–6.
- [20] Javad Sabzehali, Vijay K Shah, Harpreet S Dhillon, and Jeffrey H Reed. "3D placement and orientation of mmWave-based UAVs for guaranteed LoS coverage". In: *IEEE Wireless Communications Letters* (2021).
- [21] Fatih Yürekli and Tolga Girici. "Optimal Precoding and Deployment of Millimeter-Wave Drone Base Stations". In: *2021 International Balkan Conference on Communications and Networking (BalkanCom)*. IEEE. 2021, pp. 26–30.

- [22] Suraj Suman, Swades De, Ranjan K Mallik, Maged Elkashlan, and Arumugam Nallanathan. "Beamforming based Mitigation of Hovering Inaccuracy in UAV-Aided RFET". In: *IEEE Transactions on Communications* (2021).
- [23] Akram Al-Hourani, Sithamparanathan Kandeepan, and Abbas Jamalipour. "Modeling air-to-ground path loss for low altitude platforms in urban environments". In: *2014 IEEE global communications conference*. IEEE. 2014, pp. 2898–2904.
- [24] 3GPP. "Spatial channel model for multiple input multiple output (MIMO) simulations (3GPP TR 25.996)". In: *[Online] www.3gpp.org* (2020).
- [25] Shu Sun, Theodore S Rappaport, Mansoor Shafi, Pan Tang, Jianhua Zhang, and Peter J Smith. "Propagation models and performance evaluation for 5G millimeter-wave bands". In: *IEEE Transactions on Vehicular Technology* 67.9 (2018), pp. 8422–8439.
- [26] Lisi Jiang and Hamid Jafarkhani. "Multi-user analog beamforming in millimeter wave MIMO systems based on path angle information". In: *IEEE Transactions on Wireless Communications* 18.1 (2018), pp. 608–619.
- [27] Mihai Enescu. *5G New Radio: A Beam-based Air Interface*. John Wiley & Sons, 2020.
- [28] Jaehyun Park and Stephen Boyd. "A semidefinite programming method for integer convex quadratic minimization". In: *Optimization Letters* 12.3 (2018), pp. 499–518.
- [29] Nuwan Ganganath, Chi-Tsun Cheng, and K Tse Chi. "Data clustering with cluster size constraints using a modified k-means algorithm". In: *2014 International Conference on Cyber-Enabled Distributed Computing and Knowledge Discovery*. IEEE. 2014, pp. 158–161.
- [30] Chen Qiu, Zhiqing Wei, Xin Yuan, Zhiyong Feng, and Ping Zhang. "Multiple UAV-mounted base station placement and user association with joint fronthaul and backhaul optimization". In: *IEEE Transactions on Communications* 68.9 (2020), pp. 5864–5877.
- [31] Dilip Bethanabhotla, Ozgun Y Bursalioglu, Haralabos C Papadopoulos, and Giuseppe Caire. "User association and load balancing for cellular massive MIMO". In: *2014 Information Theory and Applications Workshop (ITA)*. IEEE. 2014, pp. 1–10.
- [32] Maurice Clerc and James Kennedy. "The particle swarm-explosion, stability, and convergence in a multidimensional complex space". In: *IEEE transactions on Evolutionary Computation* 6.1 (2002), pp. 58–73.

AUTHORS



Tolga Girici received his B.S. degree from the Middle East Technical University, Ankara, Turkey in 2000 and a Ph.D. degree from University of Maryland, College Park in 2007, both in electrical engineering. In 2005, he has spent six months as an intern at the Intelligent Automation Inc, Rockville, MD USA. He was a research assistant at the Fujitsu Labs, College Park MD USA in 2006-2007. He is currently an associate professor at TOBB University of Economics and Technology, Ankara, Turkey. He received a TUBITAK Career Award in 2010, and actively collaborates with industry. He is a senior member of IEEE. His research interests include resource allocation and optimization in next generation cellular wireless access networks, wireless ad hoc networks, smart grid and tactical networks.



Fatih Yürekli graduated from the Turkish Army Academy, Ankara, Turkey as Gendarmerie Lieutenant in 1998. He worked at different Gendarmerie units as communication and information system company commander and branch manager. Between 2016-2020 he was a chief of R&D and Project Management Branch in the Turkish Gendarmerie General Command and during this period he worked on jamming and anti-drone systems. He is currently a colonel and works as deputy commander of Şanlıurfa Province of Gendarmerie.